BBA - Bioenergetics 1864 (2023) 149002

Contents lists available at ScienceDirect

BBA - Bioenergetics

journal homepage: www.elsevier.com/locate/bbabio

Optically detected magnetic resonance and mutational analysis reveal significant differences in the photochemistry and structure of chlorophyll *f* synthase and photosystem II

Alessandro Agostini [a,b], Gaozhong Shen [c], Donald A. Bryant [c], John H. Golbeck [c,d], Art van der Est [e], Donatella Carbonera [a,*]

[a] Department of Chemical Sciences, University of Padova, Via Marzolo, 1, 35131, Padova, Italy
[b] Biology Centre, Czech Academy of Sciences, Institute of Plant Molecular Biology, Branišovská 31, 370 05 Ceske Budejovice, Czech Republic
[c] Department of Biochemistry and Molecular Biology, The Pennsylvania State University, University Park, 16802, USA
[d] Department of Chemistry, The Pennsylvania State University, University Park, 16802, USA
[e] Department of Chemistry, Brock University, 1812 Sir Isaac Brock, Way, St. Catharines, ON L2S 3A1, Canada

ARTICLE INFO

Keywords:
Chlorophyll *f*
Opticaly detected magnetic resonance
Triplet state
Type-II photosystem

ABSTRACT

In cyanobacteria that undergo far red light photoacclimation (FaRLiP), chlorophyll (Chl) *f* is produced by the ChlF synthase enzyme, probably by photo-oxidation of Chl *a*. The enzyme forms homodimeric complexes and the primary amino acid sequence of ChlF shows a high degree of homology with the D1 subunit of photosystem II (PSII). However, few details of the photochemistry of ChlF are known. The results of a mutational analysis and optically detected magnetic resonance (ODMR) data from ChlF are presented. Both sets of data show that there are significant differences in the photochemistry of ChlF and PSII. Mutation of residues that would disrupt the donor side primary electron transfer pathway in PSII do not inhibit the production of Chl *f*, while alteration of the putative Chl_Z, P680 and Q_A binding sites rendered ChlF non-functional. Together with previously published transient EPR and flash photolysis data, the ODMR data show that in untreated ChlF samples, the triplet state of P680 formed by intersystem crossing is the primary species generated by light excitation. This is in contrast to PSII, in which ^{3}P680 is only formed by charge recombination when the quinone acceptors are removed or chemically reduced. The triplet states of a carotenoid (^{3}Car) and a small amount of ^{3}Chl *f* are also observed by ODMR. The polarization pattern of ^{3}Car is consistent with its formation by triplet energy transfer from Chl_Z if the carotenoid molecule is rotated by 15° about its long axis compared to the orientation in PSII. It is proposed that the singlet oxygen formed by the interaction between molecular oxygen and ^{3}P680 might be involved in the oxidation of Chl *a* to Chl *f*.

1. Introduction

Photosynthetic organisms live in a wide range of environments in which the spectral range and intensity of the available light differ. Moreover, in any given environment the properties of the light can change rapidly. In recent years, understanding how these organisms adapt to changing light environments has been the focus of a great deal of research [1–3]. The use of the far-red region of the solar spectrum (700–750 nm) by oxygenic organisms living in environments with limited visible light is of particular interest because of the potential advantages this could confer to certain crops [4,5]. Two different biological solutions are available to photosynthetic organisms to enable the use of far-red illumination: 1) red-shifting of the absorption properties of commonly employed pigments by tuning their site energies and/or excitonic couplings [6–13] and 2) the synthesis and incorporation into photosystems of pigments such as chlorophyll (Chl) *d* [14–16] and Chl *f* [16–18] that absorb in the far-red region of the solar spectrum as a result of chemical derivatizations [16,19,20].

Chl *f*, in particular, is employed by diverse species of cyanobacteria that have been isolated from shaded environments such as microbial mats, soil, rock, caves, and stromatolites [21,22]. It has been shown that when these cyanobacteria are grown under far-red light, a conserved cluster of about twenty genes is up-regulated in a process known as Far-Red Light Photoacclimation (FaRLiP) [22]. This acclimation response leads to significant remodeling of the photosynthetic apparatus and to

* Corresponding author.
E-mail addresses: avde@brocku.ca (A. van der Est), donatella.carbonera@unipd.it (D. Carbonera).

https://doi.org/10.1016/j.bbabio.2023.149002
Received 29 May 2023; Received in revised form 24 July 2023; Accepted 31 July 2023
Available online 9 August 2023

Abbreviations

Car	carotenoid
Chl	chlorophyll
DCMU	3-(3,4-dichlorophenyl)-1,1-dimethylurea
FaRLiP	Far-Red Light Photoacclimation
FDMR	fluorescence detected magnetic resonance
ISC	intersystem crossing
ODMR	optically detected magnetic resonance
Pheo	pheophytin
PSII	photosystem II
T-S	triplet-minus-singlet
TR-EPR	transient electron paramagnetic resonance
TTET	triplet–triplet energy transfer
ZFS	zero field splitting

the production of Chl *f*. The FaRLiP gene cluster codes for altered versions of the core proteins of the major photosynthetic complexes that have been found to be specifically expressed under far-red light conditions. An analysis of this gene cluster revealed that the *psbA*4 gene is necessary for the synthesis of Chl *f* [23]. The corresponding gene product PsbA4 (formerly super-rogue D1 [24]) was therefore re-named as ChlF [23]. This protein is a paralog of the D1 core subunit of photosystem II (PSII) but many open questions about its structure and function remain. Because the D1/D2 heterodimer forms the core of PSII that binds the cofactors involved in the light-driven oxidation of water, it was proposed that the ChlF enzyme is a homodimer that produces Chl *f* by light-induced oxidation of Chl *a* or chlorophyllide *a*. Consistent with this hypothesis, its heterologous expression led to light-dependent production of Chl *f* in the cyanobacterium *Synechococcus* sp. PCC 7002, which is normally unable to make Chl *f* [23].

Recently, it was shown that active ChlF occurs as a homodimer when the *chlF* gene is expressed in a strain of *Synechococcus* 7002 lacking the *psbD*1 and *psbD*2 genes [25]. In a related study Trinugroho et al. have shown that in mutants in which only the *psbD*1 gene was deleted, ChlF can also form heterodimeric complexes with D2 that are capable of producing Chl *f* [26]. However, in the absence of D2, no evidence for the formation of stable complexes of ChlF with D1 could be found [25]. The high sequence similarity of ChlF with D1 (see Fig. 1A) is accompanied by a similar pigment stoichiometry in ChlF to that in PSII, with Chl *a* and pheophytin (Pheo) *a* at a ratio of ~3–4:1. Moreover, the carotenoids β-carotene and zeaxanthin were also found in the complex, with a Chl *a*:β-carotene:zeaxanthin ratio of approximately 8.3:0.5:0.4. Chl *f* was also identified in the substochiometric amount of about one to 25 to 29 Chl *a* molecules [25]. The presence or absence of the other co-factors that are found in PSII has not been shown conclusively in ChlF. However, the production of Chl *f* by the ChlF enzyme is inhibited by 3-(3,4-dichlorophenyl)-1,1-dimethylurea (DCMU), which also inhibits the function of PSII by binding to the Q_B plastoquinone site [25]. This suggests that ChlF probably binds plastoquinone acceptors analogous to Q_A and Q_B. In contrast, tyrosine Y183 in the *chlF* gene from *Chlorogloepsis fritschii* PCC 9212 which corresponds to Tyr_Z in D1 does not appear to be important for the function of ChlF, because the variant protein, ChlF (Y183F) is still able to produce Chl *f* when introduced into *Synechococcus* sp. PCC 7002 [25]. The residues known to bind P680, the accessory Chls, the non-heme iron, as well as the His ligand to Chl_Z in PSII are all conserved in ChlF. Notably, however, ChlF lacks all but one of the key C-terminal residues of PsbA that bind the water oxidation complex in PSII [23,24].

Flash photolysis of ChlF homodimers produced an absorbance change at 830 nm that decayed with a lifetime of ~817 μs and was assigned to a Chl triplet state based on the fact that it did not saturate with laser flash energies up to 80 mJ. Transient EPR (TREPR) spectroscopy at 90 K revealed that the main population of triplet states was characterized by zero-field splitting parameters D (2.71×10^{-2} cm^{-1}) and E (3.3×10^{-3} cm^{-1}) which are typical of Chl *a* [25]. The polarization patterns of triplet state EPR spectra allow the pathway by which they are formed to be determined because the population distribution in the spin sublevels is different for different pathways. Thus, the pattern obtained from intersystem crossing (ISC) is markedly different from that resulting from radical pair recombination [28–30]. In ChlF, the main

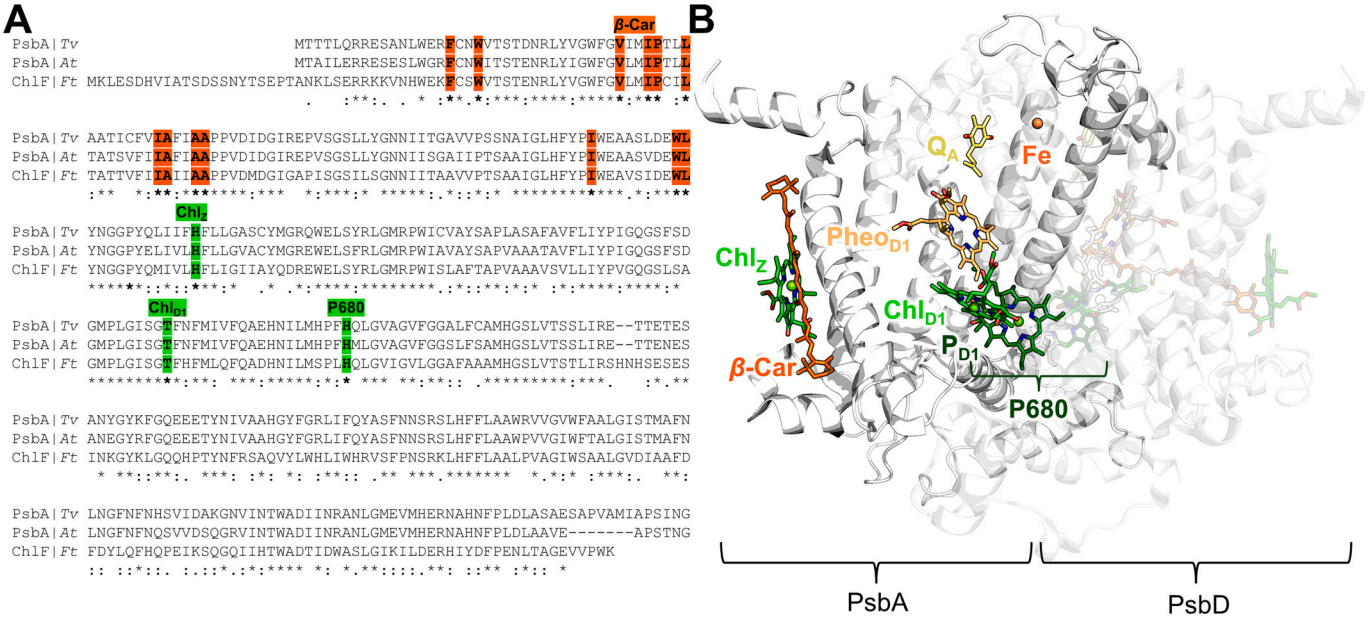

Fig. 1. A) Sequence alignment of the ChlF protein from *Fischerella thermalis* (*Ft*) (UniProtKB: G6FME5) with PsbA/D1 proteins from *Thermostichus vulcanus* (*Tv*) *and Arabidopsis thaliana* (*At*) (UniProtKB: P51765.1 and NP_051039.1, respectively). Conserved amino acids involved in the binding of chlorophyll *a*nd carotenoid are highlighted in green and orange, respectively. B) Structural model of PSII core components from *Thermostichus vulcanus* (PDB 3WU2 [27]). PsbA and PsbD are shown in cartoon format in white. Other components: dark green, P680 dimer; green, other Chls *a*; beige, Pheo *a*; orange, β-carotene; yellow, plastoquinones; red, non-heme iron atom. For clarity, only PsbA (D1) pigments are labelled and the PsbD (D2) half is semi-transparent.

population of triplet states was clearly generated by ISC. A very small contribution of a triplet state generated from radical pair recombination was also included in the simulation of the experimental spectrum, which was ascribed to a trace amount of PSI in the sample.

This behavior is very different from that observed in the isolated D1/D2 reaction center (RC) complex of PSII, which is expected to be the closest analogue of ChlF. In such complexes, the triplet state of P680 is formed by charge recombination from $P680^{+}Pheo^{-}$ in high yield upon illumination at low temperature [31,32] because the quinones are lost during the isolation procedure [33]. In the ChlF complexes, no EPR spectrum associated with charge-separated states were observed, except a very weak signal from a small amount of PSI impurity, and the triplet state is formed by ISC. From the TREPR data reported in ref. [25] it is unclear whether the triplet spectrum is from the P680 analogue, some other Chl species or if several triplet states are formed. There are also weak features in the wings of the spectrum that suggest that additional triplet states possibly from a carotenoid or Chl *f* are formed. An optically detected magnetic resonance (ODMR) investigation of ChlF opens up the possibility of assigning the triplets to specific molecular species by correlating the optical properties to the triplet population selected by the resonant conditions at specific microwave frequencies.

In this work we exploit ODMR for investigating the nature of the triplet states that are populated in the ChlF enzyme. Moreover, we investigate its properties by studying the activities of additional point mutants of ChlF. Together the results show that a triplet species very similar to ^{3}P680 in PSII is present in ChlF and that mutation of the His ligands that binds P680 abolishes Chl *f* synthesis. In addition, the ODMR data show that a carotenoid triplet state is present and could be formed by triplet-triplet energy transfer from Chl_Z. Thus, the data provide evidence that Chl_Z may be important for ChlF function, and its binding site is probably structurally similar to the corresponding site in PSII.

2. Experimental methods

2.1. Construction and analysis of site-specific variants of ChlF

Site-specific variants of the ChlF protein were produced essentially as described by Shen et al. [25]. Briefly, the *chlF* gene of *Fischerella thermalis* PCC 7521 was subcloned into plasmid pUC19, and a pair of partially complementary mutagenic primers were designed to alter the codon for the specific amino acid residue substitution that was desired. Polymerase chain reaction (PCR) amplification was performed using Q5 Hot-Start High Fidelity DNA polymerase (New England Biolabs, Ipswich, MA, USA). The amplified DNA was added directly to a kinase-ligase-*Dpn*I enzyme mixture for rapid circularization and removal of the unmodified template DNA. Following transformation into *Escherichia coli* and colony screening, plasmid DNA was isolated and sequenced to verify that only the desired mutation was present. The mutated *chlF* gene was then cloned into the pAQ1Ex-PcpcBA expression vector (conferring gentamicin resistance), which was transformed into *Synechococcus* sp. PCC 7002 for heterologous expression as previously described [23,25,34]. Pigment extraction and analysis by reversed-phase high-performance liquid chromatography (HPLC), polyacrylamide gel electrophoresis in the presence of sodium dodecylsulfate (SDS-PAGE), and immunoblotting were performed as previously described [25].

2.2. Expression and purification of ChlF

A *Synechococcus* sp. PCC 7002 strain devoid of PSII activity and heterologously expressing the *chlF* gene from the FaRLiP strain *F. thermalis* PCC 7521 was constructed by transformation of *Synechococcus* sp. PCC 7002 *ΔpsbD1*::*aadA* (Sp^R) *ΔpsbD2*::*aphAII* (Km^R) with the expression vector pAQ1Ex::$chlF^{7521}$ (carrying the *aacC* gene conferring Gm^R) [25]. Cells (9 L; ~32 g cells, wet weight) were grown photoheterotrophically at reduced light intensity (~5 μmol photons m^{-2} s^{-1}) in A^+ medium [35] supplemented with 20 mM glycerol and three antibiotics: gentamycin (50 μg • ml^{-1}), spectinomycin (100 μg • ml^{-1}) and kanamycin (100 μg • ml^{-1}).

For purification of ChlF, cells were harvested by centrifugation, washed once, and resuspended in N-2-hydroxyethylpiperazine-N′-2-ethanesulfonic acid (HEPES) buffer (50 mM HEPES, pH = 7, 10 mM $CaCl_2$, 10 mM $MaCl_2$). Cell lysis was achieved by three passages through a chilled French pressure cell at 120 MPa. After removal of unbroken cells and large cell debris by low-speed centrifugation (6500 *g*), total membranes were pelleted by ultracentrifugation (126,000 *g*) and were resuspended in the membrane buffer (50 mM HEPES, pH = 7, 300 mM NaCl, 10 % glycerol, 1 mM L-histidine and 5 μM protease inhibitor cocktail (Sigma-Aldrich, St. Louis, MO)). Membranes were diluted to 0.6 mg Chl • ml^{-1} in membrane buffer and were solubilized by addition of n-dodecyl-β-D-maltoside (β-DM) to a final concentration of 1 % (*w/v*). Insoluble debris was removed by centrifugation at 25,000 *g*. The solubilized total membrane solution was diluted two-fold with membrane buffer and loaded onto a Ni-NTA resin column pre-equilibrated with membrane buffer. The column was washed with eight column volumes of membrane buffer containing 5 mM L-histidine and 0.03 % (*w/v*) β-DM. The ChlF protein was eluted with membrane buffer containing 50 mM L-histidine and 0.03 % (w/v) β-DM. The eluted ChlF protein was dialyzed against protein purification buffer (50 mM HEPES, pH = 7, 10 mM $MgCl_2$, 10 mM $CaCl_2$, and 0.03 % (*w/v*) β-DM) and concentrated using Amicon Ultra 15 centrifugal concentration devices (30,000 MWCO; MilliporeSigma, Burlington, MA, USA). To achieve better purity by removing residual contaminating PSI, the concentrated ChlF protein solution was loaded onto 5–15 % (*w/v*) sucrose gradient and resolved by ultracentrifugation at 108,000 *g*. The upper green band containing ChlF was collected, dialyzed against the protein purification buffer, and concentrated. The purified ChlF protein was analyzed by SDS-PAGE and immunoblotting assay using an anti-ChlF antibody as described. The properties of the purified ChlF fraction were consistent with those previously reported [25]. The ChlF protein sample was aliquoted into cryotubes and stored at −80 °C until used.

2.3. ODMR experiments

Glycerol, previously degassed by several cycles of freezing and pumping, was added (60 % *v*/v) to the sample in order to obtain a transparent matrix. The glycerol was added just before the insertion into the cryostat to avoid sample degradation [36]. The sample was inserted into the cryostat pre-cooled at 60 K, in order to rapidly freeze the solution and to obtain a homogeneous and transparent matrix, and subsequently quickly cooled to 1.8 K.

ODMR spectra were acquired in a home-built set-up that has been previously reported in detail [36–38]. The principle of the ODMR technique has been described extensively in several reviews [39,40] and is also summarized in Scheme S1 in the Supporting Information. Briefly, light from a halogen lamp (250 W) is focused on the sample cell, which is immersed in a bath helium cryostat (all measurements were carried out at a temperature of 1.8 K), after being filtered through either a 5-cm $CuSO_4$ solution (FDMR spectra) or a 10-cm water filter (triplet–minus-singlet, T-S, absorption-detected spectra). In FDMR experiments, the fluorescence is detected through bandpass filters (characterized by a full width at half maximum of about 10 nm) using a photodiode placed at 90° with respect to the excitation light direction, while in absorption-detected experiments, the light transmittance is detected with standard straight geometry through a monochromator (Jobin Yvon, mod. HR250) using the same photodiode employed for the FDMR measurements. By sweeping the microwave frequency (MW source HP8559b, sweep oscillator equipped with a HP83522s plug-in and amplified by a TWT Sco-Nucletudes mod 10–46-30 amplifier) while detecting the fluorescence changes at specific wavelengths, the resonance transitions between spin sublevels of the triplet states can be determined. The microwaves are on/off amplitude-modulated for selective amplification, and the signal from the detector is demodulated and amplified using a

lock-in amplifier (EG&G, mod 5210). The analog output is connected to a computer-controlled, analog-to-digital converter. The microwave resonator, where the sample cell is inserted, consists of a slow pitch helix. FDMR spectra are presented as ΔF/F versus microwave frequency, where ΔF is the fluorescence change induced by the resonant microwave field and F is the steady-state fluorescence detected by the photodiode at the selected wavelength.

Reconstruction of the experimental FDMR spectra has been obtained following a global deconvolution analysis with Gaussian components. Fitting parameters were a) center frequencies, b) linewidth and c) relative amplitude. Errors have been determined as part of the global fitting procedure.

Once the resonance frequencies of the transitions have been determined (from the FDMR spectra, for example), microwave-induced T-S spectra can be collected by fixing the microwave frequency at a resonant value and sweeping the absorption detection wavelength [41]. T-S spectra are presented as ΔI/I versus wavelength, where ΔI is the transmittance change induced by the resonant microwave field at a certain wavelength, and I is the steady-state transmittance detected by the photodiode. It can be demonstrated [42] that for small ΔI, ΔI/I is proportional to the absorbance change induced by the resonant microwave field (i.e., ΔA). Compared to optical time-resolved absorbance spectroscopy on the triplet state, the ODMR technique allows selection (by the resonant microwave field) of specific triplet populations present in the sample, and thus well resolved T-S spectra associated with specific chromophores can be obtained.

3. Results

3.1. Analysis of site-specific variants

The similarities between ChlF and PsbA of PSII suggest that ChlF synthase likely produces Chl *f* by light-induced oxidation of Chl *a* or chlorophyllide *a*. However, the location of the active site is not known or indeed whether the electron transfer pathway is similar to that in PSII. In a previous study [25] it was shown that mutation of Tyr183, the tyrosine equivalent of Tyr_Z in PsbA, in *C. fritschii* PCC 9212 ChlF did not inhibit Chl *f* synthesis. This result suggests that Tyr_Z might not participate in electron transfer in ChlF and hence that the electron transfer pathway in ChlF may be different. To test this hypothesis further, we have constructed additional site-specific variants of ChlF in which the conserved analogues of key residues in PsbA have been altered. Because the previous study also showed that expression of the *chlF* gene from *F. thermalis* PCC 7521 resulted in greater Chl *f* production after heterologous expression, the additional site-specific variants were constructed and analyzed using the *chlF* gene from *F. thermalis* PCC 7521. Fig. S1 shows a sequence alignment of three ChlF proteins and the three PsbA sequences of *T. vulcanus*. Residues H140, Y183, H240, S288, E357, and Y361 were selected for mutagenesis in the *chlF* gene of *F. thermalis* PCC 7521. Pigments from each *Synechococcus* sp. PCC 7002 strain producing a variant ChlF protein were extracted and analyzed by reversed-phase HPLC (for examples, see Figs. S2 and S3). If a variant was unable to synthesize Chl *f*, then whole-cell protein extracts were analyzed by SDS-PAGE followed by immunoblotting. Immunoblotting showed that variant ChlF proteins were produced in all strains that were unable to produce Chl *f* (Fig. S4).

Table 1 summarizes the information obtained for the variants that were constructed, the functions of the targeted residues in PSII, and whether the ChlF variants were able to produce Chl *f*. Fourteen variants were constructed, and they clearly separated into two groups: variants that could and could not produce Chl *f*. Similar to the previous results for ChlF from *C. fritschii* PCC 9212, the Y183F variant of the *F. thermalis* PCC 7521 protein was able to produce Chl *f*, although perhaps slightly less efficiently than the WT protein. Similarly, variants in residues E357 and Y361, which are in the vicinity of, or provide ligands to, the $Mn_4Ca_1O_5$ cluster in PsbA of PSII, produced ChlF variants that could synthesize Chl *f* at least as well or in some cases with even higher yields that the wild-type protein (Table 1). When the His residue homologous to the ligand to the Chl *a* of P680 was mutated to any of five other residues (T, Y, Q, N, L), none of the resulting proteins could synthesize Chl *f* when produced in *Synechococcus* sp. PCC 7002. Similarly, when the His residue homologous to the ligand to Chl_Z, a Chl *a* molecule, was mutated to Y, L, or N, none of the resulting variants was able to synthesize Chl *f* when produced in *Synechococcus* sp. PCC 7002. Finally, a S288T variant, which should have an alteration in the plastoquinone binding site according to the structure of PsbA in PSII, did not produce Chl *f* when produced in *Synechococcus* sp. PCC 7002.

Table 1
Production of Chl *f* by site-specific variants of ChlF when produced in *Synechococcus* sp. PCC 7002.

Residue[a]	Function in PSII	Variant	Chl *f* synthesis[b]
His 140	Ligand to Chl_Z	WT	+++
		H140T	–
		H140L	–
		H140N	–
Tyr 183	Tyr_Z	WT	+++
		Y183F	++
His 220	Ligand to P680 Chl	WT	+++
		H220T	–
		H220Y	–
		H220Q	–
		H220N	–
		H220L	–
Ser 288	PQ binding	WT	+++
		S288T	–
Glu 357	Mn Cluster binding site	WT	+++
		E357L	+++
		E357Q	+++++
Tyr 361	Mn Cluster binding site	WT	+++
		Y361F	++++
		Y361H	+++

[a] See Figs. 1 and S1.
[b] A larger number of plus signs indicates higher levels of Chl *f* detected in an equal amounts of cells.

3.2. ODMR studies

Illumination of purified ChlF at 1.8 K leads to the formation of triplet states that can be detected by monitoring the change in the fluorescence/absorption induced by resonant microwaves. The strongest FDMR signals detected in the sample were those originating from triplet states of Chl *a* (^{3}Chl *a*). Three distinct ^{3}Chl *a* pools are populated showing partially resolved |D|-|E| transitions and less well resolved |D|+|E| transitions (Fig. 2, Table 2). The strongest component is characterized by zero-field splitting (ZFS) parameters |D| and |E| (0.0286 cm^{-1} and 0.0041 cm^{-1}, respectively) very close to those previously assigned to the recombination triplet of PSII (^{3}P680) detected in D1/D2 particles [32,36,43]. A negative sign of the FDMR signals is observed for a minor component when detected at short emission wavelength (670 nm).

The T-S spectrum obtained upon pumping at a frequency of 735 MHz (Fig. 3), corresponding to the ^{3}Chl a_1 |D|-|E| transition, exhibits a strong bleaching at 680 nm with a positive peak at about 672 nm and small negative bands at 636 and 626 nm, displaying a profile striking similar to that of ^{3}P680 in isolated PSII D1/D2 particles [32,44]. The band at 460 nm and the flat weak positive absorption in the entire displayed range, are assigned to triplet-triplet transitions typical of Chl triplet states [41,45].

When the microwave frequency is set at higher values (760/770/775 MHz), weaker T-S spectra are detected with broader positive and negative contributions (Fig. 4), likely due to the other two components ^{3}Chl $a_{2/3}$ observable in the FDMR spectra with opposite sign. Note that in the T-S spectra the relative contribution of the three triplets may be different compared to that of the FDMR spectra, because in the latter the

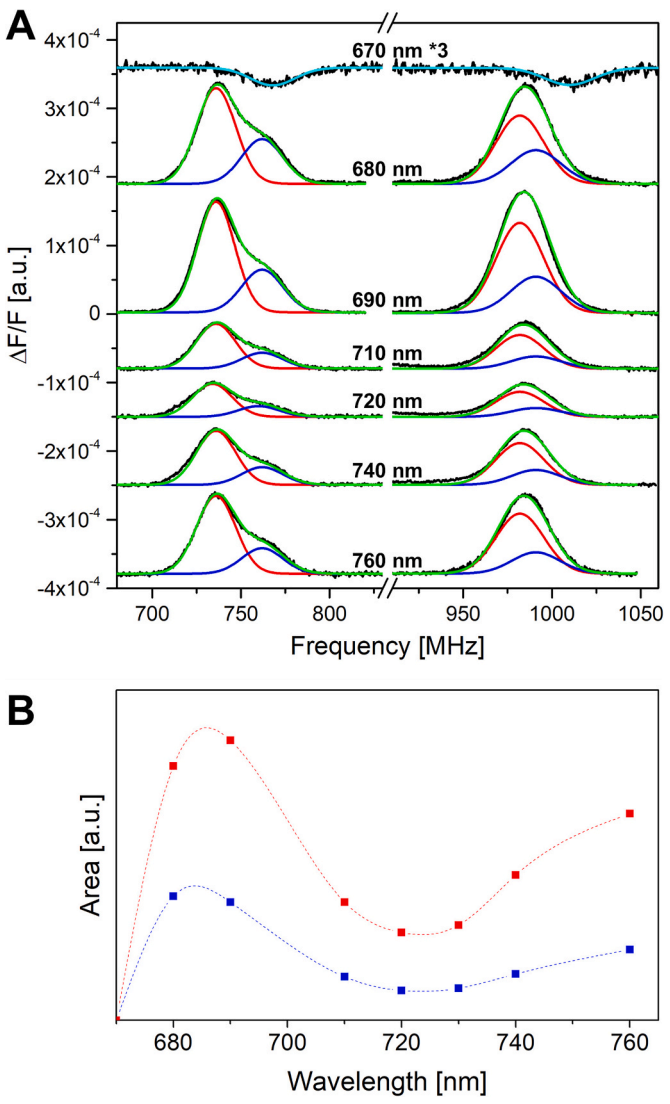

Fig. 2. ^{3}Chl *a* FDMR spectra of ChlF. ^{3}Chl *a* FDMR spectra of ChlF. (A) |D|+|E| and |D|-|E| transitions of the FDMR spectra (black lines) of ^{3}Chl *a* detected at different wavelengths in the 680–760 nm range, as indicated. Amplitude modulation 33 Hz, time constant 100 ms, temperature 1.8 K. The spectra have been vertically shifted for better comparison, and those detected at 670 nm have been multiplied to a value of 3 to enhance their intelligibility. Reconstruction (green) of the experimental spectra with Gaussian components (red, blue, and cyan). Fitting parameters reported in Table 2. (B) Amplitude dependence (averaged area of the corresponding Gaussian components fitting the |D|+|E| and |D|-|E| transitions) of the ^{3}Chl a_1 and ^{3}Chl a_2 components on the detection wavelength.

Table 2
Fitting parameters used for the reconstruction of the ^{3}Chl *a* FDMR spectra in Fig. 2.

	|D|-|E|		|D|+|E|			
	Peak [MHz]	FWHM [MHz]	Peak [MHz]	FWHM [MHz]	|D| [cm^{-1}]	|E| [cm^{-1}]
^{3}Chl a_1	736 ± 1	22 ± 1	982 ± 1	27 ± 1	0.0286 ± 0.0001	0.00410 ± 0.00005
^{3}Chl a_2	762 ± 1	23 ± 1	991 ± 1	28 ± 1	0.0292 ± 0.0001	0.00381 ± 0.00005
^{3}Chl a_3	768 ± 1	25 ± 1	1010 ± 1	28 ± 1	0.0296 ± 0.0001	0.00403 ± 0.00005

intensity is due not only to the triplet concentration but also to the emission properties of the emitters and to the energy transfer pathways, involving the Chl carrying the triplet state [46].

In addition to the signals assigned to ^{3}Chl *a*, weaker contributions were also present that we attributed to ^{3}Chl *f*. These FDMR spectra show |D|-|E| and |D|+|E| peak positions at 600 and 905 MHz, respectively, corresponding to D and E parameters of 0.0251 cm^{-1} and 0.0051 cm^{-1} (Fig. 5). The signals are not visible when detecting FDMR at 690 nm and are intense at 720 nm, meaning that they are detected from the fluorescence of a red emitter. No literature data are available for ^{3}Chl *f*, but the similar pigment Chl *d* has been reported to possess a |D| value of its triplet state smaller than that of ^{3}Chl *a* (0.0254 cm^{-1} and 0.0289 cm^{-1} for ^{3}Chl *d* and ^{3}Chl *a* in MeTHF, respectively [47]), leading to |D|-|E| and |D|+|E| transitions at frequencies (616 MHz and 906 MHz [47]), similar to those of the weak triplet signal observed in our ChlF sample.

The assignment of the FDMR signals to ^{3}Chl *f* is corroborated by considering the T-S spectra collected by pumping the microwaves at 600 and 905 MHz, which show bleaching at wavelengths (710–715 nm) that can be attributed to the Q_y absorption bands of Chl *f* (Fig. 5).

The ODMR and TREPR spectra of ChlF indicate that carotenoid triplet states (^{3}Car) are also formed when the protein is illuminated at low temperature. This behavior is different from D1/D2 particles [48–50] and single crystals of PSII complexes [51], in which only ^{3}P680 is observed. However, carotenoid triplet states have been observed in the ODMR data from PSII core complexes [52]. Fig. 6 shows the FDMR spectra detected in the microwave frequency region typical of the 2|E| transition of carotenoid triplets (maximum at 220 MHz). Carotenoid triplet states are detectable by monitoring the fluorescence of Chl, since a change in carotenoid triplet population induced by the microwave resonant field may lead to a change in the optical properties of the Chls connected to carotenoids via energy transfer [37]. The assignment is supported by the T-S spectrum detected at 220 MHz, showing the intense triplet – triplet positive absorption bands in the 500–550 nm region, and the corresponding, blue-shifted negative band due to singlet bleaching. A similar spectrum has been detected before in CP43 and CP47 and assigned to β-carotene [53].

4. Discussion

The results of the site-specific variant studies presented above suggest that, despite the sequence similarities between ChlF and PsbA, there are significant differences in their photochemistries. In PSII, P680$^+$ produced by photo-induced charge separation is reduced by electrons that are transferred from the Mn cluster via Tyr_Z. However, as shown previously [25], and confirmed here, alteration of Tyr 183 in ChlF has little effect on the synthesis of Chl *f*. Table 1 shows that mutations of residues corresponding to those that bind the Mn cluster in PSII also did not lead to a loss of Chl *f* production. This region of the protein differs significantly between PSII and ChlF. However, the results shown in Table 1, indicate that it does not play a functional role since single mutations of Tyr183, Glu357 and Tyr361 do not disrupt Chl *f* synthesis. Thus, we can conclude that the active site is probably not located on the lumenal side of ChlF in the part of the protein corresponding to the water oxidation site of PSII. In contrast, mutation of the His ligands to the P680 chlorophyll, prevents Chl *f* synthesis. Similarly, mutation of Ser288 in the PQ binding region also produces loss of function. This indicates an involvement of P680 and possibly PQ in the process.

In PSII, the Chl_Z molecule bound by PsbD is part of an alternative electron transfer pathway that donates electrons to P680$^+$ via Car bound by PsbD when the primary pathway from the Mn cluster to P680$^+$ is blocked [54,55]. This suggests that Chl_Z might have a functional role in ChlF. Mutation of His140 in ChlF, which corresponds to the axial ligand to Chl_Z in PsbA of PSII, completely abolishes Chl *f* synthesis. Thus, we can conclude that Chl_Z does indeed play an important role in the function of ChlF and could potentially be the Chl *a* that is oxidized to Chl *f*. We note, however, that the Chl_Z bound to PsbA in PSII does not play any

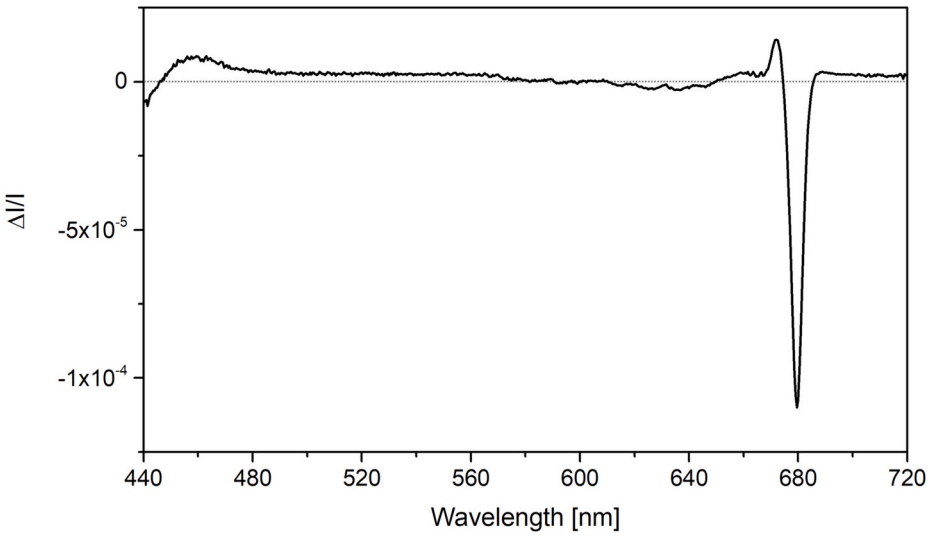

Fig. 3. ^{3}Chl *a* T-S spectra of ChlF. T-S spectrum of the most intense ^{3}Chl *a* component. Resonance frequency 735 MHz, amplitude modulation 33 Hz, time constant 1 s, temperature 1.8 K.

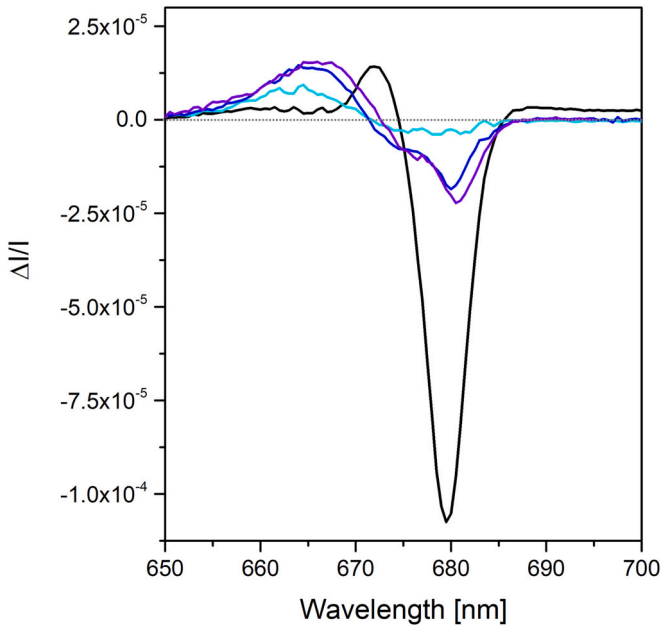

Fig. 4. ^{3}Chl *a* T-S spectra of the various resonance frequencies: 735 MHz (black line), 760 MHz (purple line), 770 MHz (blue line), and 775 MHz (cyan line). Amplitude modulation 33 Hz, time constant 1 s, temperature 1.8 K.

known functional role, and thus its involvement in the photochemistry would be specific to ChlF.

The ODMR data reveal that several triplet states are formed, the main population being assignable to a cofactor reminiscent of P680, on the basis of the ZFS parameters and of the associated T-S spectrum both of which are similar to those detected in the isolated D1D2Cytb_{559} RC [32]. However, unlike the PSII RC case, the main ^{3}Chl *a* observed in ChlF is not populated by charge recombination but by ISC, as revealed by the previous EPR results and independently confirmed here [25]. This is an unexpected result because in PSII ^{3}P680 is only formed by charge recombination of $P680^{+}Pheo^{-}$ when the quinone acceptors are removed or chemically reduced. In contrast, in ChlF the previously reported transient absorbance data and TREPR data, and ODMR data presented here, show that ^{3}P680 is formed by ISC. Thus, together with the mutation result showing that alteration of Tyr_{Z} has little effect on the function, the data indicate that the photochemistry in ChlF is notably different from that in PSII.

By using $^{18}O_2$, Chen and coworkers showed that two ^{18}O atoms were incorporated into the newly synthesized Chl *f*, indicating that the oxygen in the formyl group of Chl *f* is derived from molecular oxygen (together with the oxygen introduced into the isocyclic ring by AcsF) [56]. Thus, our finding of a species similar to ^{3}P680 that is formed in the complex by ISC is a unique feature of the ChlF RC-like system and may be relevant to explain the photo-oxidation of Chl *a* to Chl *f*, because Chl triplet states are known to produce reactive singlet oxygen species in high yield [57,58].

The weaker contribution to the FDMR that we attributed to ^{3}Chl *f* may be explained as a population of Chl *f* that remains weakly bound to the complex after its synthesis (note that Chl *f* is present in a sub-stoichiometric amount [25]). The site(s) where these Chl *f* molecules are bound cannot be identified from the ODMR data but are likely to be far from the carotenoid because triplet quenching would occur if they were nearby. Because the residues involved in binding the carotenoids in PSII are conserved in ChlF, a similar structure and location for the carotenoid is likely (see Fig. S5). We speculate that the enzyme active site should be reachable from the P680 binding site, if the singlet oxygen produced by its triplet state plays a functional role in the Chl *a* to Chl *f* conversion. This, together with the mutation study, points towards the Chl_{Z} site as a possible location. If the structure of ChlF is similar to that of PsbA, as strongly suggested from the high homology, the capability of the carotenoid to form a triplet state is likely due to the quenching of the Chl triplet state populated in the Chl_{Z} site (Fig. 1), because it is the only Chl close enough to the carotenoid in the complex, while other ^{3}Chls *a*, especially ^{3}P680, are unquenched. Because ^{3}Cars are not populated directly from their excited singlet states, due to the intrinsic low probability of ISC, the presence of ^{3}Car means that triplet-triplet-energy-transfer from ^{3}Chl, is active in ChlF. It is noteworthy that this photoprotective mechanism seems to be selectively directed to the quenching of a specific Chl, since, as shown above, several unquenched ^{3}Chls are formed in the protein complex. Weak features in the wings of the TREPR spectrum reported by Shen et al. were tentatively assigned to a carotenoid triplet, although they were not included in the fitting [25]. We repeated the fit of the TREPR spectrum reported in Shen et al. with a ^{3}Chl *a* contribution characterized by an ISC polarization [59,60] and a ^{3}Car contribution for which the triplet sublevel population rates were adjusted to fit the experimental TREPR spectrum (see Fig. S6). Because the ^{3}Car spin polarization patterns depend on the relative orientation of the donor-acceptor triplet-triplet energy transfer (TTET) pair, as it is

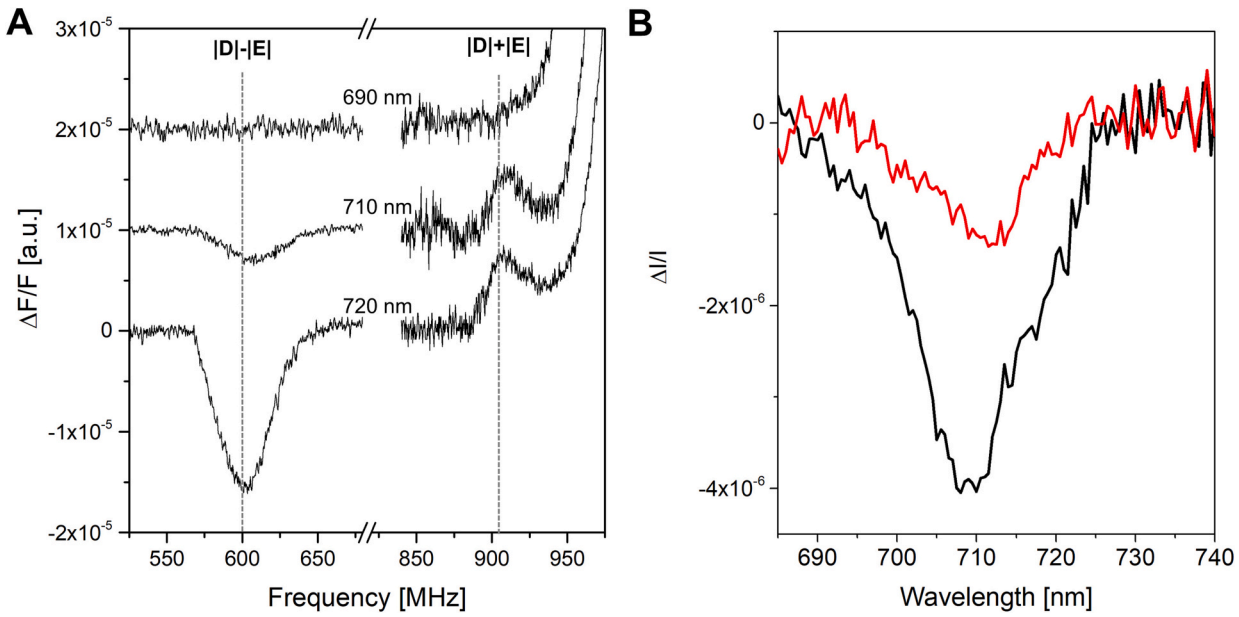

Fig. 5. ^{3}Chl *f* ODMR spectra of ChlF. (A) ^{3}Chl *f* FDMR spectra of ChlF. |D|+|E| and |D|-|E| transitions of the FDMR spectra of ^{3}Chl *f* detected at different wavelengths in the 690–720 nm range, as indicated. Amplitude modulation 33 Hz, time constant 100 ms, temperature 1.8 K. The spectra have been vertically shifted for better comparison. Vertical dashed lines highlight the |D|-|E| and |D|+|E| peak positions (600 and 905 MHz, respectively). (B) T-S spectrum of ^{3}Chl *f* at 600 MHz (black line) and 905 MHz (red line). Amplitude modulation 33 Hz, time constant 1 s, temperature 1.8 K.

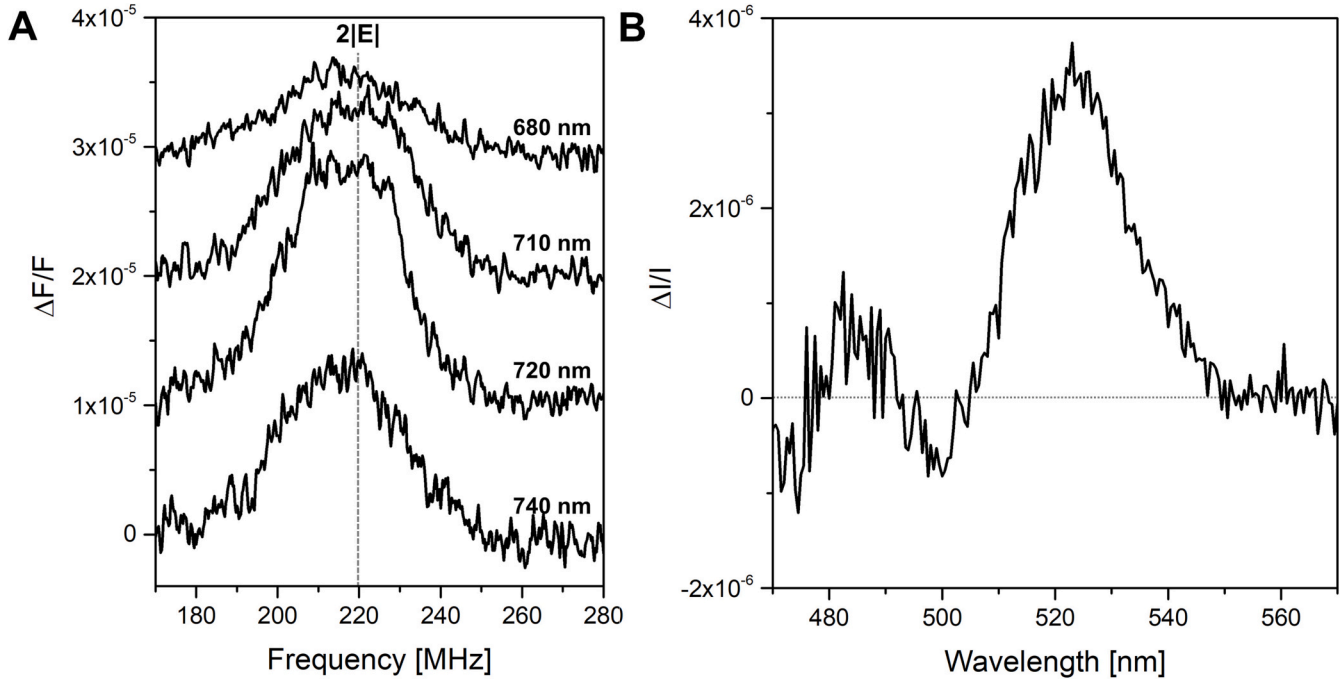

Fig. 6. ^{3}Car ODMR spectra of ChlF. (A) 2|E| transitions of the FDMR spectra of ^{3}Chl *f* detected at different wavelengths in the 680–740 nm range, as indicated. Amplitude modulation 333 Hz, time constant 100 ms, temperature 1.8 K. The spectra have been vertically shifted for better comparison. Vertical dotted line highlights 2|E| peak position (220 MHz). (B) T-S spectrum of ^{3}Car. Resonance frequency 220 MHz, amplitude modulation 333 Hz, time constant 1 s, temperature 1.8 K.

inherited from the ^{3}Chl donor during TTET in a way that is determined by the pigment arrangement inside the protein scaffold [61,62], it was possible to determine which Chl-Car pair was compatible with the ^{3}Car polarization obtained in the fit (see supporting information for more details). The only Chl-Car pair with π-π distance compatible with a TTET mechanism [61] in *T. vulcanus* PsbA [27] is Chl_Z and the β-Car (see Figs. 1B and S5B). However, the relative orientation of the Chl-Car pair in PsbA is not compatible with the experimentally determined ^{3}Car polarization in ChlF, suggesting that the two chromophores are oriented differently in ChlF. We found that a 15° rotation of the carotenoid along its long axis is sufficient to reproduce the observed polarization pattern. Because the β-Car is bound in a conserved groove (see Fig. S1A), this relatively subtle difference is reasonable and can be considered to be likely. Thus, the ability of the carotenoid to quench the Chl_Z triplet state

may be instrumental to preventing photodamage until the oxidation to Chl *f* occurs. Once formed, Chl *f* would presumably move from this site for incorporation into the photosystems. The fact that we detected a population of ^{3}Chl *f* that is not quenched by Car is consistent with this scenario.

5. Conclusions

The data presented here demonstrate that there are significant differences in the primary photochemistry of PSII and ChlF despite their apparent sequence similarity. The mutational analysis shows that residues that are expected to inactivate the donor side primary electron transfer pathway do not inhibit Chl *f* production. Together, the ODMR and previously published TREPR data show that the triplet state of P680 is formed by ISC in ChlF samples. This contrasts with PSII complexes in which electron transfer between P680 and Pheo out-competes ISC and hence ^{3}P680 can only be formed by charge recombination after reduction or removal of the quinones. Clearly a difference in the light-induced events is present but further study is needed to unravel fully the primary photochemistry. We suggest that the tendency to form ^{3}P680, which is able to induce the formation of $^{1}O_2$, might be instrumental to the conversion reaction of Chl *a* into Chl *f*, which is known to depend on both O_2 and light. The fact that mutation of the axial His ligand to Chl_Z abolishes Chl *f* production and the evidence for quenching of the Chl_Z triplet state by the nearby carotenoid both point to Chl_Z as a likely candidate for oxidation to Chl *f*.

CRediT authorship contribution statement

Conceptualization, DAB, JHG, AvdE, and DC; Data curation, AA; Formal analysis, AA, GS, DAB, AdvE, and DC; Funding acquisition, AA, DAB, AvdE, and DC; Investigation, AA and GS; Methodology, AA and GS; Project administration, DC; Resources, DAB and DC; Supervision, DAB and DC; Visualization AA; Writing - original draft, AA, GS, DAB, AvdE, and DC; Writing - review & editing, all authors.

Declaration of competing interest

The authors declare that they have no known competing financial interests or personal relationships that could have appeared to influence the work reported in this paper.

Data availability

Data will be made available on request.

Acknowledgements

A.A. and D.C. gratefully acknowledge financial support by the University of Padova (P-DiSC-2019). A.A. acknowledges the institutional support of RVO: 60077344 and the MEMOVA project, EU Operational Programme Research, Development and Education No. CZ.02.2.69/0.0/0.0/18_053/0016982. D.A.B and J.H.G. gratefully acknowledge support from the U.S. National Science Foundation (grant MCB-1613022). A.v.d.E. acknowledges support from the Natural Science and Engineering Research Council, Canada (Discovery Grant, 2015-04021).

Appendix A. Supplementary data

Supplementary data to this article can be found online at https://doi.org/10.1016/j.bbabio.2023.149002.

References

[1] M. Chen, Chlorophyll modifications and their spectral extension in oxygenic photosynthesis, Annu. Rev. Biochem. 83 (2014) 317–340.
[2] F. Gan, D.A. Bryant, Adaptive and acclimative responses of cyanobacteria to far-red light, Environ. Microbiol. 17 (2015) 3450–3465.
[3] A.V. Pinevich, S.G. Averina, On the edge of the rainbow: red-shifted chlorophylls and far-red light photoadaptation in cyanobacteria, Microbiology. 91 (2022) 631–648.
[4] R.E. Blankenship, M. Chen, Spectral expansion and antenna reduction can enhance photosynthesis for energy production, Curr. Opin. Chem. Biol. 17 (2013) 457–461.
[5] M. Chen, R.E. Blankenship, Expanding the solar spectrum used by photosynthesis, Trends Plant Sci. 16 (2011) 427–431.
[6] B.M. Wolf, R.E. Blankenship, Far-red light acclimation in diverse oxygenic photosynthetic organisms, Photosynth. Res. 142 (2019) 349–359.
[7] E. Kotabová, J. Jarešová, R. Kaňa, R. Sobotka, D. Bína, O. Prášil, Novel type of red-shifted chlorophyll *a* antenna complex from *Chromera velia*. I. Physiological relevance and functional connection to photosystems, Biochim. Biophys. Acta Bioenerg. 1837 (2014) 734–743.
[8] D. Bína, Z. Gardian, M. Herbstová, E. Kotabová, P. Koník, R. Litvín, O. Prášil, J. Tichý, F. Vácha, Novel type of red-shifted chlorophyll *a* antenna complex from *Chromera velia*: II, Biochemistry and spectroscopy, Biochim. Biophys. Acta - Bioenerg. 1837 (2014) 802–810.
[9] R. Litvín, D. Bína, M. Herbstová, M. Pazderník, E. Kotabová, Z. Gardian, M. Trtílek, O. Prášil, F. Vácha, Red-shifted light-harvesting system of freshwater eukaryotic alga *Trachydiscus minutus* (Eustigmatophyta, Stramenopila), Photosynth. Res. 142 (2019) 137–151.
[10] T. Morosinotto, J. Breton, R. Bassi, R. Croce, The nature of a chlorophyll ligand in Lhca proteins determines the far red fluorescence emission typical of photosystem I, J. Biol. Chem. 278 (2003) 49223–49229.
[11] E. Romero, M. Mozzo, I.H.M. van Stokkum, J.P. Dekker, R. van Grondelle, R. Croce, The origin of the low-energy form of photosystem I light-harvesting complex Lhca4: mixing of the lowest exciton with a charge-transfer state, Biophys. J. 96 (2009) L35–L37.
[12] F. Passarini, E. Wientjes, H. van Amerongen, R. Croce, Photosystem I light-harvesting complex Lhca4 adopts multiple conformations: red forms and excited-state quenching are mutually exclusive, Biochim. Biophys. Acta Bioenerg. 1797 (2010) 501–508.
[13] M. Kosugi, M. Kawasaki, Y. Shibata, K. Hara, S. Takaichi, T. Moriya, N. Adachi, Y. Kamei, Y. Kashino, S. Kudoh, H. Koike, T. Senda, Uphill energy transfer mechanism for photosynthesis in an Antarctic alga, Nat. Commun. 14 (2023) 730.
[14] H. Miyashita, H. Ikemoto, N. Kurano, K. Adachi, M. Chihara, S. Miyachi, Chlorophyll *d* as a major pigment, Nature. 383 (1996) 402.
[15] H. Schiller, H. Senger, H. Miyashita, S. Miyachi, H. Dau, Light-harvesting in *Acaryochloris marina* - spectroscopic characterization of a chlorophyll *d*-dominated photosynthetic antenna system, FEBS Lett. 410 (1997) 433–436.
[16] F. Gan, S. Zhang, N.C. Rockwell, S.S. Martin, J.C. Lagarias, D.A. Bryant, Extensive remodeling of a cyanobacterial photosynthetic apparatus in far-red light, Science 345 (2014) 1312–1317.
[17] M. Chen, Y. Li, D. Birch, R.D. Willows, A cyanobacterium that contains chlorophyll *f* - a red-absorbing photopigment, FEBS Lett. 586 (2012) 3249–3254.
[18] M. Chen, M. Schliep, R.D. Willows, Z.-L. Cai, B.A. Neilan, H. Scheer, A red-shifted chlorophyll, Science 329 (2010) 1318–1319.
[19] Y. Li, M. Chen, Novel chlorophylls and new directions in photosynthesis research, Funct. Plant Biol. 42 (2015) 493.
[20] M.-Y. Ho, N.T. Soulier, D.P. Canniffe, G. Shen, D.A. Bryant, Light regulation of pigment and photosystem biosynthesis in cyanobacteria, Curr. Opin. Plant Biol. 37 (2017) 24–33.
[21] L.A. Antonaru, T. Cardona, A.W.D. Larkum, D.J. Nürnberg, Global distribution of a chlorophyll *f* cyanobacterial marker, ISME J. 14 (2020) 2275–2287.
[22] F. Gan, G. Shen, D. Bryant, Occurrence of far-red light photoacclimation (FaRLiP) in diverse cyanobacteria, Life. 5 (2014) 4–24.
[23] M.-Y. Ho, G. Shen, D.P. Canniffe, C. Zhao, D.A. Bryant, Light-dependent chlorophyll *f* synthase is a highly divergent paralog of PsbA of photosystem II, Science 353 (2016) aaf9178–aaf9178.
[24] J.W. Murray, Sequence variation at the oxygen-evolving Centre of photosystem II: a new class of 'rogue' cyanobacterial D1 proteins, Photosynth. Res. 110 (2012) 177–184.
[25] G. Shen, D.P. Canniffe, M.-Y. Ho, V. Kurashov, A. van der Est, J.H. Golbeck, D. A. Bryant, Characterization of chlorophyll *f* synthase heterologously produced in *Synechococcus* sp. PCC 7002, Photosynth. Res. 140 (2019) 77–92.
[26] J.P. Trinugroho, M. Bečková, S. Shao, J. Yu, Z. Zhao, J.W. Murray, R. Sobotka, J. Komenda, P.J. Nixon, Chlorophyll *f* synthesis by a super-rogue photosystem II complex, Nat. Plants. 6 (2020) 238–244.
[27] Y. Umena, K. Kawakami, J.-R. Shen, N. Kamiya, Crystal structure of oxygen-evolving photosystem II at a resolution of 1.9 Å, Nature. 473 (2011) 55–60.
[28] D.E. Budil, M.C. Thurnauer, The chlorophyll triplet state as a probe of structure and function in photosynthesis, Biochim. Biophys. Acta Bioenerg. 1057 (1991) 1–41.
[29] W. Lubitz, F. Lendzian, R. Bittl, Radicals, radical pairs and triplet states in photosynthesis, Acc. Chem. Res. 35 (2002) 313–320.
[30] S. Weber, Transient EPR, in: D. Goldfarb, S. Stoll (Eds.), EPR Spectrosc. Fundam. Methods, John Wiley & Sons, 2018, pp. 195–214.
[31] M.K. Bosch, I.I. Proskuryakov, P. Gast, A.J. Hoff, Time-resolved EPR study of the primary donor triplet in D1-D2-cyt b_{559} complexes of photosystem II: temperature dependence of spin−lattice relaxation, J. Phys. Chem. 100 (1996) 2384–2390.
[32] D. Carbonera, G. Giacometti, G. Agostini, A well resolved ODMR triplet minus singlet spectrum of P680 from PSII particles, FEBS Lett. 343 (1994) 200–204.
[33] P.J. van Leeuwen, M.C. Nieveen, E.J. van de Meent, J.P. Dekker, H.J. van Gorkom, Rapid and simple isolation of pure photosystem II core and reaction center particles from spinach, Photosynth. Res. 28 (1991) 149–153.

[34] Y. Xu, R.M. Alvey, P.O. Byrne, J.E. Graham, G. Shen, D.A. Bryant, in: R. Carpentier (Ed.), Expression of Genes in Cyanobacteria: Adaptation of Endogenous Plasmids As Platforms for High-level Gene Expression in *Synechococcus* sp. PCC 7002, 2011, pp. 273–293. Photosynth. Res. Protoc.
[35] M. Ludwig, D.A. Bryant, Transcription profiling of the model cyanobacterium *Synechococcus* sp. strain PCC 7002 by next-gen (SOLiDTM) sequencing of cDNA, Front. Microbiol. 2 (2011).
[36] S. Santabarbara, E. Bordignon, R.C. Jennings, D. Carbonera, Chlorophyll triplet states associated with photosystem II of thylakoids, Biochemistry. 41 (2002) 8184–8194.
[37] D. Carbonera, G. Giacometti, G. Agostini, FDMR of carotenoid and chlorophyll triplets in light-harvesting complex LHCII of spinach, Appl. Magn. Reson. 3 (1992) 859–872.
[38] A. Agostini, D.M. Palm, H. Paulsen, D. Carbonera, Optically detected magnetic resonance of chlorophyll triplet states in water-soluble chlorophyll proteins from *Lepidium virginicum*: evidence for excitonic interaction among the four pigments, J. Phys. Chem. B 122 (2018) 6156–6163.
[39] D. Carbonera, Optically detected magnetic resonance (ODMR) of photoexcited triplet states, Photosynth. Res. 102 (2009) 403–414.
[40] E. Goovaerts, Optically detected magnetic resonance (ODMR), in: EMagRes, John Wiley & Sons, Ltd, Chichester, UK, 2017, pp. 343–358.
[41] A.J. Hoff, Optically detected magnetic resonance (ODMR) of triplet states, in: J. Amesz, A.J. Hoff (Eds.), Advances in Photosynthesis and Respiration vol. 3, Kluwer Academic Publishers, Dordrecht, 1996. Biophysical Techniques in Photosynthesis.
[42] H.J. Den Blanken, R.F. Meiburg, A.J. Hoff, Polarized triplet-minus-singlet absorbance difference spectra measured by absorbance detected magnetic resonance. An application to photosynthetic reaction centers, Chem. Phys. Lett. 105 (1984) 336–342.
[43] S. Santabarbara, G. Agostini, A.P. Casazza, C.D. Syme, P. Heathcote, F. Böhles, M. C.W. Evans, R.C. Jennings, D. Carbonera, Chlorophyll triplet states associated with photosystem I and photosystem II in thylakoids of the green alga *Chlamydomonas reinhardtii*, Biochim. Biophys. Acta Bioenerg. 1767 (2007) 88–105.
[44] R. van der Vos, P.J. van Leeuwen, P. Braun, A.J. Hoff, Analysis of the optical absorbance spectra of D1-D2-cytochrome *b*-559 complexes by absorbance-detected magnetic resonance, Biochim. Biophys. Acta Bioenerg. 1140 (1992) 184–198.
[45] J. Vrieze, A.J. Hoff, The orientation of the triplet axes with respect to the optical transition moments in (bacterio) chlorophylls, Chem. Phys. Lett. 237 (1995) 493–501.
[46] G.F.W. Searle, T.J. Schaafsma, Fluorescence detected magnetic resonance of the primary donor and inner core antenna chlorophyll in photosystem I reaction centre protein: Sign inversion and energy transfer, Photosynth. Res. 32 (1992) 193–206.
[47] M. Di Valentin, S. Ceola, G. Agostini, A. Telfer, J. Barber, F. Böhles, S. Santabarbara, D. Carbonera, The photo-excited triplet state of chlorophyll *d* in methyl-tetrahydrofuran studied by optically detected magnetic resonance and time-resolved EPR, Mol. Phys. 105 (2007) 2109–2117.
[48] Y. Takahashi, Ö. Hansson, P. Mathis, K. Satoh, Primary radical pair in the photosystem II reaction Centre, Biochim. Biophys. Acta Bioenerg. 893 (1987) 49–59.
[49] J.R. Durrant, L.B. Giorgi, J. Barber, D.R. Klug, G. Porter, Characterisation of triplet states in isolated photosystem II reaction centres: oxygen quenching as a mechanism for photodamage, Biochim. Biophys. Acta Bioenerg. 1017 (1990) 167–175.
[50] J. Niklas, A. Agostini, D. Carbonera, M. Di Valentin, W. Lubitz, Primary donor triplet states of photosystem I and II studied by Q-band pulse ENDOR spectroscopy, Photosynth. Res. 152 (2022) 213–234.
[51] M. Kammel, J. Kern, W. Lubitz, R. Bittl, Photosystem II single crystals studied by transient EPR: the light-induced triplet state, Biochim. Biophys. Acta Bioenerg. 1605 (2003) 47–54.
[52] S. Santabarbara, A. Agostini, A.P. Casazza, G. Zucchelli, D. Carbonera, Carotenoid triplet states in photosystem II: coupling with low-energy states of the core complex, Biochim. Biophys. Acta Bioenerg. 2015 (1847) 262–275.
[53] D. Carbonera, G. Giacometti, G. Agostini, A. Angerhofer, V. Aust, ODMR of carotenoid and chlorophyll triplets in CP43 and CP47 complexes of spinach, Chem. Phys. Lett. 194 (1992) 275–281.
[54] C.A. Tracewell, A. Cua, D.H. Stewart, D.F. Bocian, G.W. Brudvig, Characterization of carotenoid and chlorophyll photooxidation in photosystem II, Biochemistry. 40 (2001) 193–203.
[55] J. Wang, D. Gosztola, S.V. Ruffle, C. Hemann, M. Seibert, M.R. Wasielewski, R. Hille, T.L. Gustafson, R.T. Sayre, Functional asymmetry of photosystem II D1 and D2 peripheral chlorophyll mutants of *Chlamydomonas reinhardtii*, Proc. Natl. Acad. Sci. 99 (2002) 4091–4096.
[56] H. Garg, P.C. Loughlin, R.D. Willows, M. Chen, The $C2^1$-formyl group in chlorophyll *f* originates from molecular oxygen, J. Biol. Chem. 292 (2017) 19279–19289.
[57] A.A. Krasnovskii Jr., Singlet molecular oxygen: mechanisms of formation and paths of deactivation in photosynthetic systems, Biofizika. 39 (1994) 236–250.
[58] H. Küpper, R. Dědic, A. Svoboda, J. Hala, P.M. Kroneck, Kinetics and efficiency of excitation energy transfer from chlorophylls, their heavy metal-substituted derivatives, and pheophytins to singlet oxygen, Biochim. Biophys. Acta - Gen. Subj. 1572 (2002) 107–113.
[59] A. Agostini, L. Nicol, N. Da Roit, M. Bortolus, R. Croce, D. Carbonera, Altering the exciton landscape by removal of specific chlorophylls in monomeric LHCII provides information on the sites of triplet formation and quenching by means of ODMR and EPR spectroscopies, Biochim. Biophys. Acta Bioenerg. 1862 (2021), 148481.
[60] M. Di Valentin, F. Biasibetti, S. Ceola, D. Carbonera, Identification of the sites of chlorophyll triplet quenching in relation to the structure of LHC-II from higher plants. Evidence from EPR spectroscopy, J. Phys. Chem. B 113 (2009) 13071–13078.
[61] M. Di Valentin, D. Carbonera, The fine tuning of carotenoid–chlorophyll interactions in light-harvesting complexes: an important requisite to guarantee efficient photoprotection via triplet–triplet energy transfer in the complex balance of the energy transfer processes, J. Phys. B Atomic Mol. Phys. 50 (2017), 162001.
[62] D. Carbonera, M. Di Valentin, C. Corvaja, G. Giacometti, G. Agostini, P.A. Liddell, A.L. Moore, T.A. Moore, D. Gust, Carotenoid triplet detection by time-resolved EPR spectroscopy in carotenopyropheophorbide dyads, Photochem. Photobiol. 105 (1997) 329–335.